Composites Science and Technology 214 (2021) 108955

Contents lists available at ScienceDirect

Composites Science and Technology

journal homepage: www.elsevier.com/locate/compscitech

Control of Mullins stress softening in silicone elastomer composites by rational design of fumed silica fillers

Vincent Allen [a], Lunhan Chen [a,d], Milena Englert [a], Aziz Moussaoui [a], Wojciech Pisula [a,b,c,*]

[a] Evonik Operations GmbH, Rodenbacher Chaussee 4, 63457 Hanau-Wolfgang, Germany
[b] Max Planck Institute for Polymer Research, Ackermannweg 10, 55128 Mainz, Germany
[c] Department of Molecular Physics, Faculty of Chemistry, Lodz University of Technology, Zeromskiego 116, 90-924 Lodz, Poland
[d] Department of Chemistry, RWTH Aachen University, Landoltweg 1, 52074 Aachen, Germany

ARTICLE INFO

Keywords:
Silicone elastomers
Fumed silica
Reinforcement
Fatigue behavior
Mullins effect

ABSTRACT

The influence of fumed silica as reinforcement filler is investigated on the Mullins stress softening in composite silicone elastomers. Especially, the impact of surface area, loading level, surface chemistry, and structure modification of fumed silica is evaluated on the fatigue behavior of high consistency silicone rubber. It is observed that high loading level and large surface area of fumed silica increase the energy loss during initial loading cycles which is related to disruptions in filler-polymer interactions. Addition of a processing aid or hydrophobization of the silica surface decrease the brittleness and energy loss of the compounds. A close correlation between Shore A hardness and energy loss is found confirming the contribution of the filler-polymer interactions on Mullins stress-softening. At the same time, the permanent set remains almost independent of the surface hydrophobicity of the filler indicating a breakdown of the structured silica agglomerates during initial deformation. To improve the fatigue resistance of the silicone elastomer, a structure modified and hydrophobic silica, AEROSIL® R 8200, was used leading to the lowest permanent set even at high loading levels in combination with good mechanical reinforcement. The reduction in energy loss and permanent set is attributed to the combination of hydrophobic surface and low aggregate structure of the silica preventing agglomerate breakdown and chain disentanglements at the silica surface. This study provides fundamental understanding on the relation between filler-polymer interactions, filler morphology and Mullins stress softening for the rational design of future filler particles in reinforced elastomer composites with improved fatigue resistance.

1. Introduction

Elastomers are viscoelastic materials which can extend to extreme elongations with minimal plastic deformation. This elastic behavior makes elastomers ideal for applications requiring dynamic loadings and sealing behavior [1]. Silicone rubber, described by a molecular backbone of -Si-*O*- repeating units, is an organosilicon elastomer commonly found in applications requiring high temperature ranges and high chemical inertness [2]. Despite the higher temperature resistance than organic rubbers due to the -Si-*O*- backbone with a bonding energy of 466 kJ/mol, silicone elastomers have relatively weak mechanical properties because of poor intermolecular forces between the polymer chains [3]. To improve these low mechanical properties, reinforcement of the elastomer is necessary by small particle fillers such as synthetic silica [4,5].

Synthetic silica, which is the filler of choice for silicone elastomers due to its great compatibility and retention of optical transparency, is an amorphous silicon dioxide which can be produced in an aqueous solution, for precipitated silica, or via a flame hydrolysis process, for fumed silica [6]. The significant differences in production processes for fumed and precipitated silicas result in completely different silica aggregate morphologies. Precipitated silica is based on amorphous, low structured, porous and three-dimensionally clustered aggregates [7], and fumed silica consists of amorphous, chain-like, branched aggregates [8,9]. Primarily, fumed silica is used for silicone rubber as a reinforcing agent due to its specific aggregate morphology leading to a higher reinforcement that is defined as the increase in tensile strength, tear resistance, abrasion resistance and modulus above expected values based on Einstein-Guth and Gold theory [10]. The effects of reinforcement are dependent on polymer and filler types, and the degree of dispersion of

* Corresponding author. Evonik Operations GmbH, Rodenbacher Chaussee 4, 63457, Hanau-Wolfgang, Germany.
E-mail address: wojciech.pisula@evonik.com (W. Pisula).

https://doi.org/10.1016/j.compscitech.2021.108955
Received 1 February 2021; Received in revised form 25 June 2021; Accepted 16 July 2021
Available online 31 July 2021

fillers in the elastomer matrix [11,12]. The following filler factors influence the reinforcement of elastomers: (1) contact area between the particle and polymer based on the primary particle size, specific surface area, and filler loading level, (2) restrictive properties of the filler based on the structure or the degree of irregularity, and (3) filler-filler and filler-polymer interactions based on the surface reactivity [13,14]. The filler-polymer interactions involve adsorption and entanglement of the chains at the filler surface [15,16].

While fumed silica is a powerful reinforcing agent, its addition induces undesirable, non-elastic behavior during dynamic testing leading to permanent deformations of the elastomer. Fatigue is described as the weakening or destruction of material due to loading. Elastomers are unique because of their viscoelastic behavior resulting in sensitivities to the type of loading, stress amplitude, strain amplitude, strain rates, loading history and the environmental conditions [17]. Due to these sensitivities, an extensive variety of fatigue testing methods exists, investigating properties like crack propagation, energy loss, and fatigue life in which Weibull distribution functions are appropriate for representing fatigue testing of rubber elastomers [18].

Compressive, shear, tensile, and torsional fatigue tests results are used to understand the effects of different polymer systems. This includes investigations into the effects of different fillers on the elastomer polymer network. Fillers, which are necessary for the reinforcement of elastomers, introduce additional effects during dynamic testing which otherwise does not occur in unfilled elastomers [19]. These effects include the Payne and Mullins effects, respectively termed after the leading contributing researchers describing these unique dynamic behaviors of filled rubber [20,21]. When measuring the response of filled elastomers in low strain amplitudes (<10%), the Payne effect can be monitored, while at medium to high strain amplitudes (>20%), the Mullins effect can be observed [22].

In silicone elastomers, the Mullins stress softening is attributed to bond rupture or slippage of chain entanglements along the filler surface of chains reaching their limit of extensibility [23,24]. Thereby, the Mullins effect is a strongly anisotropic phenomenon [25]. Uniaxial tensile preconditioning in one direction hardly causes any stress softening in the perpendicular direction. As mentioned, covalent bond scission contributes significantly to the stress softening and is highly anisotropic as proven also by mechanoluminescence of filled silicone elastomers [26]. The scission of even a small number of covalent bonds plays a discernible role in the Mullins effect of reinforced silicone elastomers. Since fatigue resistance and long-term reliability of mechanical properties are key requirements of silicone elastomers for their applications, especially in novel technologies such as soft robotics [27,28], the influence of different types of silica fillers on the Mullins stress softening needs to be well understood.

In this study, morphological factors of fumed silica are studied on thier influence on the stress softening of high consistency silicone rubber (HCR). Silica filled HCR is an ideal rubber compound for investigating fatigue damage based on filler-polymer interactions. Different grades of fumed silica varying in aggregate morphology, specific surface area and surface chemistry are in focus of this investigation to acquire fundamental information on the Mullins effect of reinforced silicone elastomers. To gain insight into these properties, cyclic stress softening tensile studies were performed on a broad number of silica fillers. The magnitude of energy loss and permanent set are used to describe the resulting stress softening in changes of filler surface area, surface chemistry, and aggregate morphology. It is observed that the fatigue resistance can be significantly improved by applying structure modified hydrophobic silica fillers.

2. Experimental

2.1. Materials

To ensure reproducibility of the results all components including the silica used in this study are commercial and globally available. The dimethylsiloxane, methyl vinyl gum with a molecular weight (M_n) of 200,000 g/mol known as BLUESIL™ GUM 751 supplied by Elkem was used as the base polymer for HCR formulations. The vinyl groups are located along the backbone with a vinyl content of 800 ppm. Hydroxyl terminated polydimethylsiloxane with a dynamic viscosity of 35–50 mPas at 25 °C was used as the processing aid. A peroxide cure agent, di (2,4-dichlorobenzoyl)peroxide, known as DCLBP-50-PSI was supplied

Table 1
Properties of AEROSIL® fumed silica used in this investigation.

Silica name (Abbreviation)	BET - specific surface area (m^2/g)	Hydrophobic (R) - structure modified (M)	Surface treatment reagent
AEROSIL® 90 (AE 90)	90	–	–
AEROSIL® 150 (AE 150)	150	–	–
AEORISL® 200 (AE 200)	200	–	–
AEROSIL® 255 (AE 255)	255	–	–
AEROSIL® 300 (AE 300)	300	–	–
AEROSIL® 380 (AE 380)	380	–	–
AEROSIL® R 104 (AE R 104)	150	R	Octamethylcyclotetrasiloxane
AEROSIL® R 106 (AE R 106)	250	R	Octamethylcyclotetrasiloxane
AEROSIL® R 812 (AE R 812)	260	R	Hexamethyldisilazane
AEROSIL® R 812 S (AE R 812 S)	220	R	Hexamethyldisilazane
AEROSIL® R 972 (AE R 972)	110	R	Dimethyldichlorosilane
AEROSIL® R 974 (AE R 974)	170	R	Dimethyldichlorosilane
AEROSIL® R 976 (AE R 976)	250	R	Dimethyldichlorosilane
AEROSIL® R 8200 (AE R 8200)	160	R - M	Hexamethyldisilazane

by United Initiators.

Fumed silica under the brand name of AEROSIL® of different surface areas, primary particle sizes, and hydrophobicities were provided by Evonik Industries AG. The properties of the fumed silica for this study are shown in Table 1. The used fumed silica is classified by its hydrophobicity (R), structure modification (M), and/or surface area. Seven of the chosen fumed silica have an unmodified hydrophilic surface, shown in Table 1 as AEROSIL® followed by the mean surface area (e.g. AEROSIL® 300 is an unmodified hydrophilic fumed silica with mean surface area of 300 m^2/g). Hydrophobic AEROSIL® are denoted using R followed by a number representative of different hydrophobization agents (see Table 1). AEROSIL® R 812 and AEROSIL® R 812 S are both surface modified AEROSIL® 300, using the hydrophobization reagent HMDS. The additional "S" represents further hydrophobization in which AEROSIL® 300 is treated with HMDS for a longer amount of time. Structure modified AEROSIL® are denoted with a four-digit number such as AEROSIL® R 8200.

2.2. Formulation

In standard HCR formulation, 100 parts per hundred (silicone) rubber (phr), 40 phr silica, and 6 phr of processing aid are used. Processing aid was used only for hydrophilic silica formulations, but not for any hydrophobic silica formulations. AEROSIL® 200 was used for investigations of variations in silica loading levels and testing the effects of processing aid. To investigate the effects of different loading levels of silica filler on dynamic properties, AEROSIL® 200 was incorporated at loading levels of 20, 30, 40, 50, and 60 phr.

A two-roll mill, Servitec Maschinenservice GmbH, was used for the processing and mixing of HCR. This processing was separated into two sections, namely silica incorporation (nip size of 0.75 cm, a roll speed of 20 rpm, friction ratio between the front and back rolls of 1.3) and cure package incorporation (seven days after first processing, nip gap of 0.95 cm, roll speed of 20 rpm, friction ratio of 1.3). A sufficient compounding time was applied to ensure consistent and uniform agglomerate sizes in the composites. After the addition of peroxide, samples were left to rest overnight before curing.

2.3. Sample preparation

To cure and prepare HCR samples for mechanical testing, a Wickert heating press was used. Puck and square shaped plaques of a respective thickness of 6 mm and 2 mm were created for the mechanical tests. The HCR compounds were cured at a temperature of 140 °C and a pressure of 130 bar. An additional post-curing step was carried out in a convection heated oven for 6 h at 200 °C. Before mechanical testing, the samples were placed in a climate-controlled room for a minimum of 3 days.

2.4. Characterization methods

2.4.1. TEM imaging

HCR filled with fumed silica were cryo-cut and imaged in a Hitachi H-7500 transmission electron microscope (TEM). The analysis of the images was performed by the software iTEM from EMSIS.

2.4.2. Hardness testing

Shore A hardness tests were performed using a SIMTEC hardness tester according to DIN 53505 standards. The average hardness of a total of 5 test points was calculated using a puck with a diameter of 50 mm and a thickness of 6 mm.

2.4.3. Tensile testing

Tensile and dynamic stress softening testing were performed using a Zwick/Roell ZO10 with a 500 N loading cell and pressurized clamps. Specimen dimensions follow ASTM D412 C standards and were created using the Zwick die cutter. Tensile tests were performed at an elongation speed of 500 mm/min with an initial 0.5 N sample loading. The nominal strain was calculated according to Equation 1 and related to the initial elongation after 0.5 N loading which was always 60 mm in length. The nominal stress was calculated according to Equation 2. For each sample, the thickness was measured and directly entered into the Zwick software to calculate the sample area. A minimum of 8 samples were used to calculate the average value for the maximum nominal stress and strain while using the crosshead displacement.

Equation 1 – nominal strain

$$\varepsilon = \frac{\Delta I}{I_0}$$

Equation 2 – nominal stress

$$\sigma = \frac{F_{\perp}}{A}$$

2.4.4. Mullins testing

Dynamic property testing was performed according to Fig. S1. Samples were stretched to an initial elongation of 50% in the first cycle and returned to a minimum load of 0.5 N. Every consecutive cycle increased elongation by a value of 50% until the specimen breaks. Using a loading/unloading elongation speed of 500 mm/min, the maximum stress, maximum elongation, energy loss per cycle, and permanent set were calculated.

The energy loss per cycle is calculated according to Fig. S2 where energy loss is the difference between the area between the loading and unloading curves. Energy loss was only calculated for complete cycles in which the loading and unloading curves reached the respective elongation and returned to 0.5 N force. The sum of the energy loss for each cycle results in the total energy loss as in Equation 3.

Equation 3 – total energy loss

$$E_{total} = \sum_{i=1}^{n} E_{cycle\ i}$$

Analogous to energy loss, the elongation is measured on the final complete cycle. The change in permanent set per cycle is calculated according to Equation 4. The average values are calculated for both permanent set and change in permanent set per cycle.

Equation 4 – change in permanent set

$$\Delta\varepsilon_{PS} = \left|\varepsilon_{cycle\ i+1} - \varepsilon_{cycle\ i}\right|$$

3. Results and discussion

HCR formulations were reinforced either by hydrophilic or hydrophobic silica. All formulations which use hydrophilic silica were prepared with and without a processing aid for comparison. Compounds with hydrophobic silica remain soft and do not require the addition of processing aid. Therefore, this difference in formulations is analyzed and discussed in the following results.

Regarding the mechanical properties, only the hardness of the compounds is discussed to establish a correlation to the Mullins effect. Fig. 1a depicts Shore A hardness as a function of filler loading for hydrophilic fumed silica of AE 200 with and without processing aid. With processing aid, the hardness increases in a linear fashion with loading level from 35 Shore A at 20 phr to 70 Shore A at 60 phr due to stronger polymer-particle and particle-particle interactions in the compound. This trend is in agreement with the increase of the E-modulus with loading level for precipitated silica as previously reported, whereby the tensile strength showed an optimum at a critical correlation length among aggregates [29]. Stronger interactions are observed for the compound without processing aid for which the Shore A hardness increases by a factor of 10 over the entire loading level following also an almost linear trend. The hardness depends almost linearly on the surface area of the hydrophilic fumed silica in the range from 90 m^2/g to 300

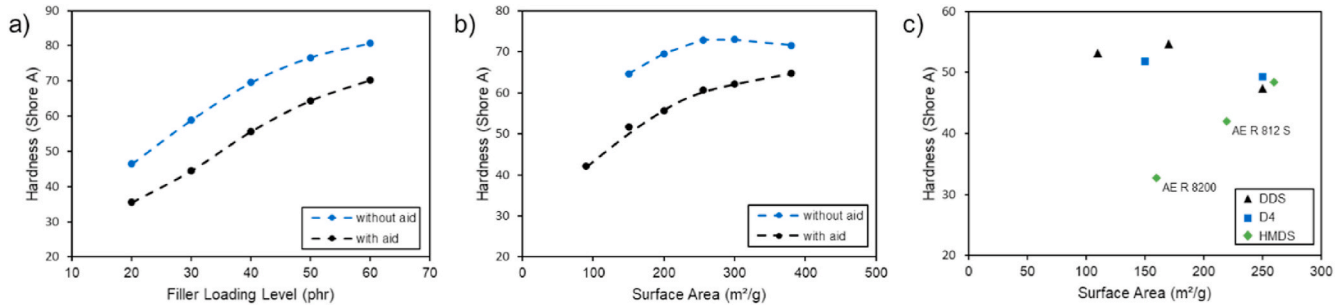

Fig. 1. a) Shore A hardness is plotted as function of loading level for hydrophilic AE 200 with and without processing aid; b) Shore A hardness as function of specific surface area for hydrophilic fumed silica with and without processing aid at filler loading level 40 phr; c) Shore A hardness as function of specific surface area for hydrophobic fumed silica at filler loading level 40 phr (data points for AE R 812 S and structure modified AE 8200 are indicated). Dashed lines are guides for the eyes only.

m^2/g for compounds filled at 40 phr silica and processing aid (Fig. 1b). The rise in hardness from 40 Shore A for 90 m^2/g to 65 Shore A for 380 m^2/g is attributed also to enhanced polymer-particle and particle-particle interactions. The total number of silanol groups capable of hydrogen bonding is significantly enlarged with higher surface area. Reported simulations revealed that silanol groups strongly interact with the PDMS backbone [30], and larger amounts of polymer is absorbed on hydrophilic silica than on treated hydrophobic silica [31]. However, at 380 m^2/g, a maximum hardness is reached implying a certain limit of polymer absorption on the silica surface. In the absence of the processing aid, the hydrogen bonding is stronger resulting in a rise of the hardness by 10 Shore A for the surface area of 150 m^2/g and by 5 Shore A for 380 m^2/g. The maximum hardness is observed in the range between 255 m^2/g and 300 m^2/g.

Modification of the silica surface hydrophobicity by protecting the silanol groups leads to predominantly weaker van-der-Waals interactions as reported in literature [32]. In this study, the purpose of the octamethylcyclotetrasiloxane (D4), dimethyldichlorosilane (DDS) and hexamethyldisilazane (HMDS) modification of the silica was to tune the surface character of the filler. In comparison to D4 and DDS, HMDS provides a higher hydrophobicity leading to lower filler-polymer interactions. As shown in Fig. 1c, the hardness remains on the level of 45–50 Shore A and is independent of the hydrophobization agent for the whole investigated surface area between 90 m^2/g to 260 m^2/g. Two exceptions are evident from the graph. The hardness of the extra hydrophobic AE R 812 S is lower than for the other studied hydrophobic silica. In this case, no remaining silanol groups are left on the surface and the weak van-der-Waals interactions dominate the hardness. The hardness of the hydrophobic structure modified AE R 8200 drops even stronger in comparison to the other hydrophobic silica. This indicates that the structure modification has a great impact when the silanol groups are covered and only van-der-Waals interactions take place. These results are in good agreement with literature confirming the influence of loading, surface area and hydrophobization of silica fillers on the hardness of silicone composites and are important for the later discussed correlations between fatigue behavior and hardness of the silicones.

Energy loss was measured at every cycle until break for all Mullins tests with each cycle increasing in elongation by 50% and is plotted as a function of elongation with each increase representing the subsequent completed cycle. Fig. 2 describes the energy loss as a function of percent elongation for AE 200 at different loading levels with and without processing aid. For both cases, the energy loss increases with higher loading levels. This stress softening is related to breaking of the existing filler-filler and filler-polymer interactions. The higher the silica loading is and the larger the network of hydrogen bonds is, the higher the energy loss during the cyclic loading. The energy loss also increases for compounds without processing aid since more interactions are established. However, these compounds become brittle at higher silica loadings

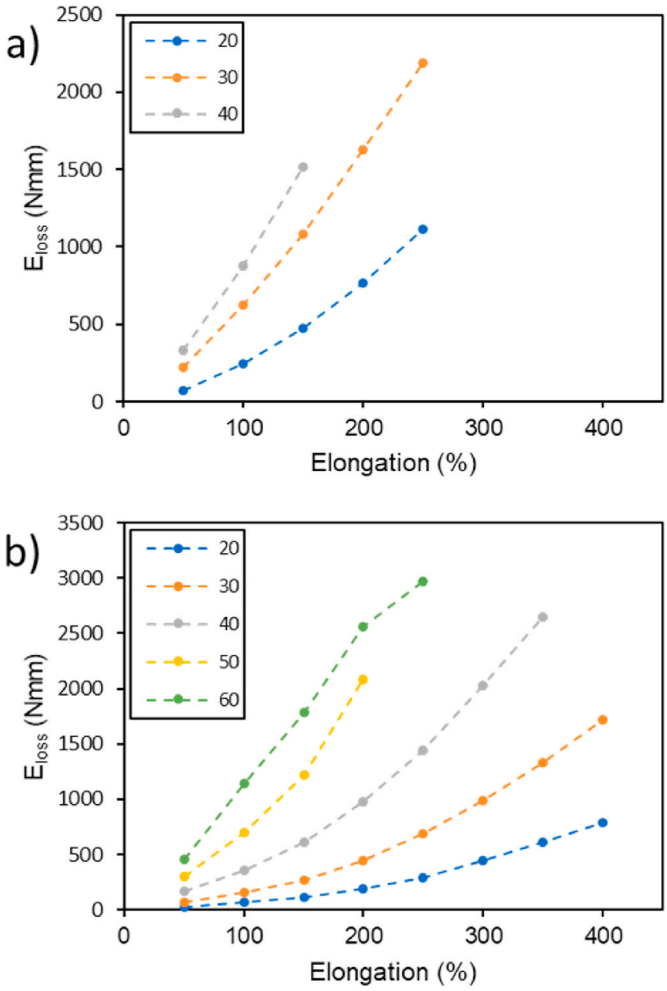

Fig. 2. Energy loss is plotted against elongation for different loading levels of AE 200 a) without and b) with processing aid. Dashed lines are guides for the eyes only.

leading to break at lower elongations and reduced number of completed measurable cycles. Therefore, the summation of energy loss of cycles 1, 2, and 3 (elongations at 50%, 100%, and 150%) are used as the energy loss value. The energy loss is also dependent on the elongation since higher energies are necessary to break all hydrogen bonds at greater elongations.

Fig. 3a depicts the total energy loss as the sum of cycles 1–3 to 150% elongation for different loading levels of AE 200. As already noted

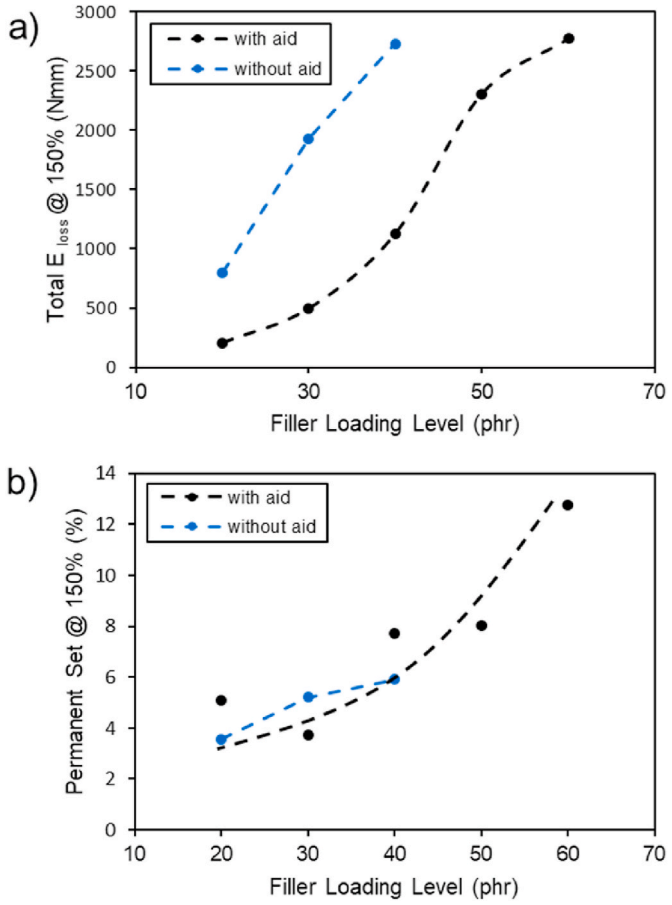

Fig. 3. a) Total energy loss and b) permanent set both at 150% elongation plotted as function of loading level for compounds with AE 200 with and without processing aid. Dashed lines are guides for the eyes only.

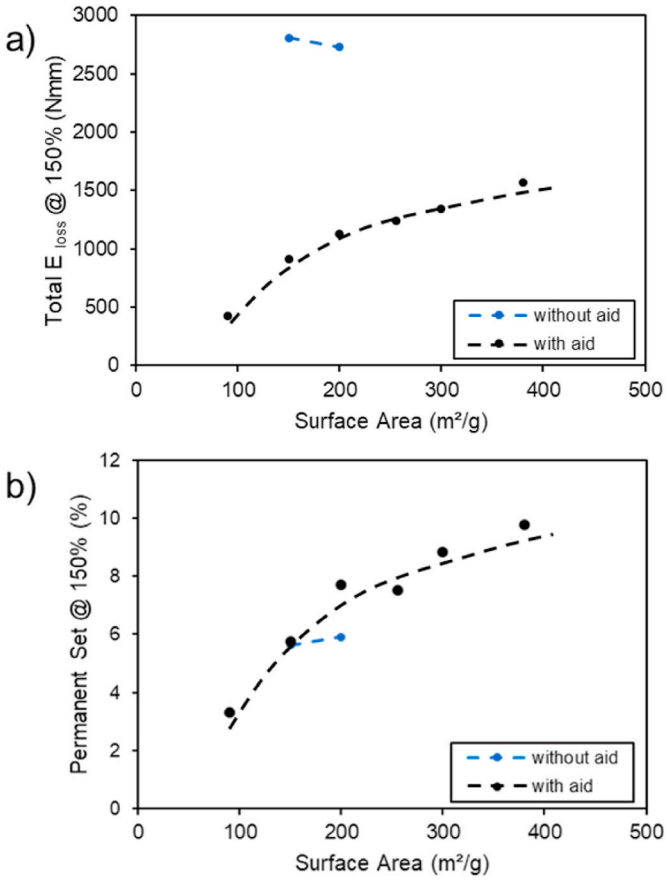

Fig. 4. a) Total energy loss and b) permanent set both at 150% elongation as function of surface area for hydrophilic fumed silica at 40 phr loading with and without processing aid. Dashed lines are guides for the eyes only.

before, there is a direct correlation with the loading level and energy loss. The energy loss increases with higher loading level for compounds with and without processing aid. The energy loss without the aid is significantly higher by up to 1500 Nmm at AE 200 loading of 30 phr. This confirms that a higher energy is required for breaking more hydrogen bonding. Compounds with more than 40 phr silica were too brittle to perform the 3 cycles and showed break before 150% elongation.

Permanent set at 150% elongation was measured in unison with energy loss during Mullins testing. The permanent set on the completion of cycle 3 is plotted as a function of loading level for compounds with AE 200 in Fig. 3b. Similar to the trend of energy loss, the increase in filler loading level in compounds with processing aid leads to a larger permanent set. A higher permanent set indicates stronger ruptures in the filler-filler and filler-polymer interactions during tensile strain, possibly including more pronounced polymer chain slippage along the filler and disentanglement of polymer chains. Interestingly, the compounds without processing aid reveal a permanent set on identical level indicating that similar breakage occurs during tensile strain.

Fig. 4 depicts the total energy loss and permanent set at 150% elongation as a function of surface area for compounds filled with hydrophilic fumed silica, with and without processing aid. As observed for the Shore A hardness (Fig. 1b), energy loss and permanent set for compounds without processing aid strongly increase for lower surface areas and tend to reach a constant value at high surface areas. This trend can be explained again by increased filler-filler and filler-polymer interactions due to a higher number of silanol groups creating hydrogen bonding that break during elongation and result in an increase of the permanent set. Especially the amount of bound rubber increases with higher filler loading and surface area [33]. Since silica of higher surface area has larger interfacial area to the polymer matrix together with increased number of silanol groups, more chains can be adsorbed on the filler surface leading to larger distortions during stress softening. But this trend is less pronounced at higher surface areas when access to the entire filler surface by the polymer is limited. Additionally, the particle distance decreases with the increased number of fumed silica particles at higher filler loadings [34]. The compounds without processing aid reveal a ca 2.5-fold higher energy loss, which is not determinable for surface areas above 200 m^2/g due to a too high brittleness of the silicone samples. A similar behavior has been reported for other silicone types which exhibited strong viscosity increase at high filler loading of AE 200 and AE 300 [35]. Despite the significantly increased energy loss for these compounds, the permanent set is on similar level as for compounds with processing aid. This might indicate a faster recovery of the filler-polymer bond rupture in compounds without processing aid as more silanol groups are exposed for interactions. This is confirmed in Fig. 5 by the permanent set for compounds filled with hydrophobic silica which is on an identical level as for hydrophilic silica with processing aid.

As obvious from Fig. 5, the total energy loss and permanent set at 150% elongation of hydrophobic fumed silica deviate from the correlations observed for the hydrophilic filler. In comparison to compounds filled with hydrophilic fumed silica without processing aid, the energy loss of the hydrophobic dramatically drops to the level of 1250 Nmm – 1500 Nmm and remains almost independent of the surface area between 130 m^2/g – 260 m^2/g. These observations are in line with other studies reporting a decline of the stress softening for silicones filled with surface treated silica [36]. The strong decline of the energy loss is related to the

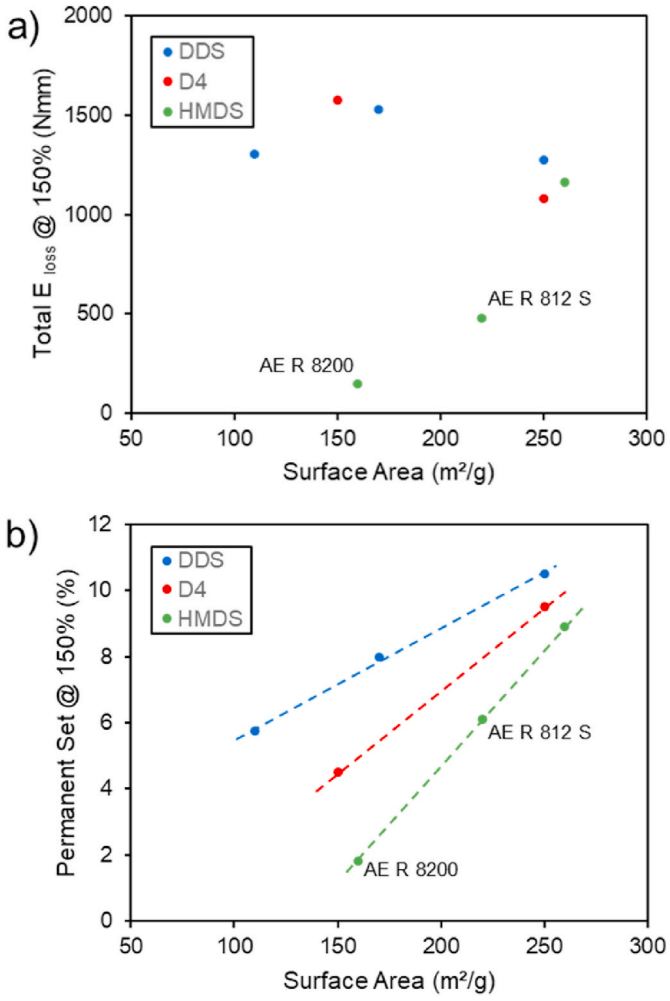

Fig. 5. a) Total energy loss and b) permanent set, both at 150% elongation and 40 phr, are plotted as function of surface area for hydrophobic fumed silica using DDS (blue), D4 (red), and HMDS (green), respectively. The data include silica with extra hydrophobicity (AE R 812 S) and structure modification (AE R 8200). (For interpretation of the references to colour in this figure legend, the reader is referred to the Web version of this article.)

methylated silanol groups inducing weak van der Waals forces. As mentioned earlier, despite the lower energy loss, the permanent set is almost identical for comparable surface areas of hydrophilic silica indicating that besides the rupture of hydrogen bonding, the particle morphology and agglomerate structure are also contributing factors. Interestingly, the stronger hydrophobized silica, AE R 812 S (indicated on the graph as "extra hydrophobic"), results in even more van der Waals forces and subsequently in the further decline of the energy loss and lower permanent set in comparison with the other hydrophobic silica of similar surface area. The largest reduction in energy loss and permanent set is observed for the structure modified and HMDS surface modified AE R 8200 (indicated in the graph as "structure modified"). While the energy loss increases with higher filling level of AE R 8200, the permanent set of the compound is independent of loading level and remains constant at low values (Fig. S3). This behavior of AE R 8200 is attributed to the combination of HMDS modification and structure modification reducing chain rupture from the silica surface thus lowering the structural damage.

To understand the influence of surface area, hydrophobicity and structure modification on silica dispersion in the silicone compound, TEM images were taken for hydrophilic silica AE 90, AE 200 and AE 300 in comparison to AE R 8200 and are shown in Fig. 6a. The light regions represent the silicone matrix and the dark regions are the silica filler. Silica with a smaller surface area such as 90 m^2/g show larger dark regions indicating larger aggregate and agglomerate sizes, while increasing the surface area improves the aggregate dispersion in the compound as evident from smaller dark regions in the case of 300 m^2/g. These images confirm a fine dispersion and closer aggregate distance of silica with high surface area in the silicone compound [35]. Interestingly, the TEM of the HCR compound with AE R 8200 discloses the most uniform distribution indicating the highest dispersion. The TEM results were further analyzed concerning the index of dispersion. As evident from Fig. 6b, the index of dispersion (I_d) only slightly improves for silica with higher specific surface area from 19.9 for AE 90 to 14.3 for AE 300. The lowest I_d of only 9.6 is found for the HCR compound with AE R 8200. Dispite its initial significantly larger particle size in comparison to AE 200 after 5 min of ultrasonification (see Table S1 for particle sizes that are 0.159 μm for AE 200 and 12.62 μm for AE R 8200), at sufficiently high shear forces during HCR compounding AE R 8200 is well dispersed presumably into much small particles due to its structure modification and hydrophobic surface.

After reviewing the results, a trend between energy loss and hardness is found. When the hardness of the silica filled compound increases, so

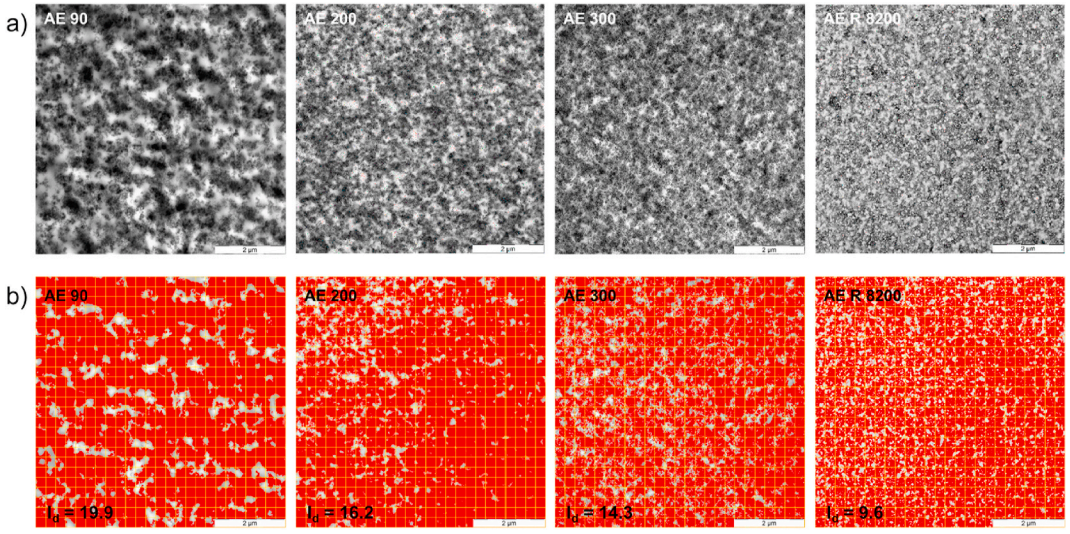

Fig. 6. a) TEM images for cryo-cut HCR compounds at loading of 40 phr filled with AE 90, AE 200, AE 300 and AE R 8200 and b) corresponding dispersion maps including the index of dispersion (I_d).

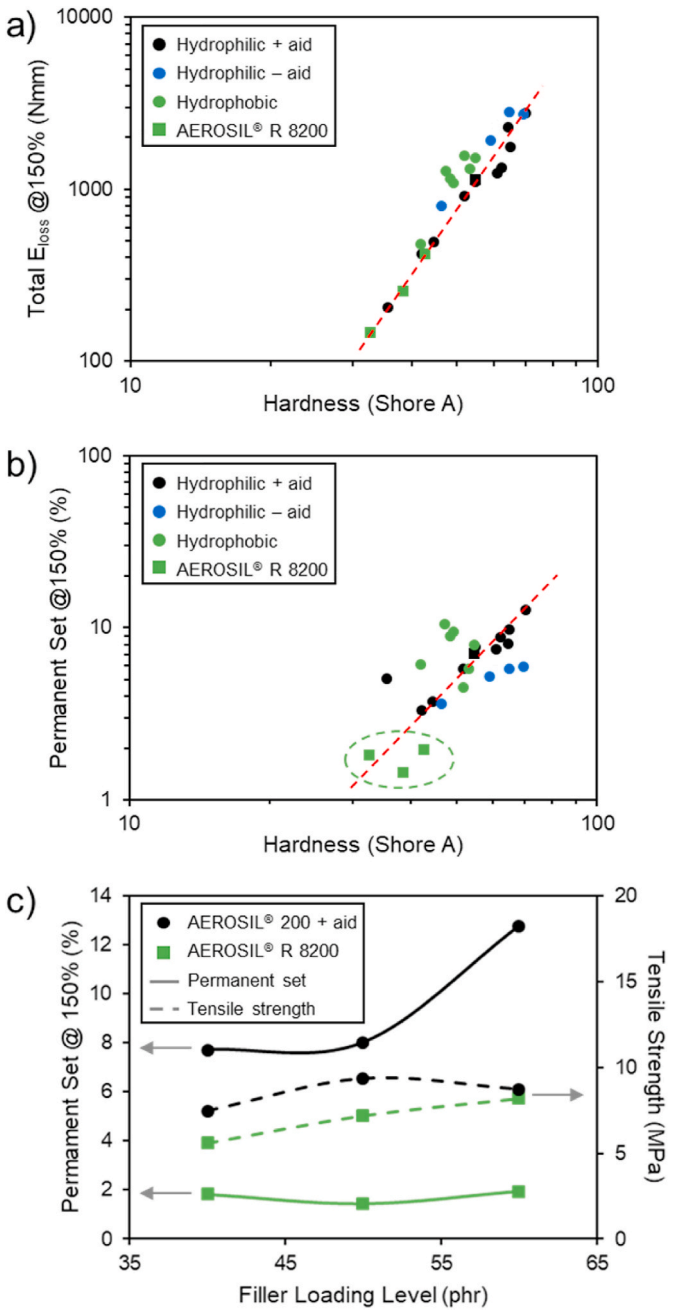

Fig. 7. a) Total energy loss and b) permanent set at 150% elongation plotted double logarithmically against hardness for all HCR compounds. AE R 8200 filled compounds are indicated by dashed circle. c) Comparison of permanent set and tensile strength of AE R 8200 and AE 200 (with processing aid) at different filling levels. Dashed lines are guides for the eyes only.

does the energy loss. Therefore, energy loss is plotted double logarithmically as a function of Shore A hardness for all investigated HCR compounds in Fig. 7a, distinguishing hydrophobic and hydrophilic fumed silica with and without processing aid. Surprisingly, independent of the silica type and additive, a close correlation between energy loss and hardness is found. A high reinforcement is related, at least partially, to the strong filler-polymer interactions which are in turn expressed by the high energy loss during initial stressing of the compound. This allows for an easy prediction of the Mullins stress softening based on the material hardness and means a low energy loss requires a trade off in material hardness. The permanent set data points are more scattered versus the hardness and do not follow a close trend as shown in Fig. 7b. It is evident that the lowest set values are obtained for compounds filled with the hydrophobic and structure modified AE R 8200 (indicated in dashed circle in the graph). Even at higher filling level the permanent set remains at a negligible level, with good reinforcement at the same time. As presented in Fig. 7c, the tensile strength of compounds filled with AE R 8200 increases gradually with higher loading level preserving a low permanent set. This would allow to apply high loadings for improved reinforcement without losing the low permanent set that is important for fatigue resistance. In contrast, compounds with AE 200 and processing aid, that are commonly applied for the reinforcement of HCR, reveal a tensile strength on identical level, but a significantly higher permanent set. While the tensile strength remains almost unchanged for different filling levels, the permanent set strongly rises.

The hydrophobic surface of AE R 8200 decreases non-covalent filler-polymer interactions, while the reduced aggregate structure prevents disruption through chain disentanglements at the silica surface. It was previously shown that especially this silica grade, AE R 8200, results in a particularly low fraction of bound rubber due to a reduced number of adsorbed chains on the hydrophobic surface and decreased amount of trapped chains within the structure modified aggregates (Fig. 8c and d) [33]. Another aspect important for the stress softening is related to the aggregate and agglomerate silica structure. It was reported that highly structured fillers tend to break apart under stress, while less structured ones show lower energy loss [37]. Recent models indicate that stress softening and high hysteresis of reinforced rubber is rather attributed to an irreversible breakdown of larger filler clusters during the first deformation cycle [38]. During deformation, the size of the clusters decreases with larger strain. It is assumed that the gaps between broken clusters are filled up with the polymer due to strong interactions to the filler surface hindering a reagglomeration after stress relaxation. These predictions are recently verified by experimental in-situ small-angle neutron and X-ray scattering [39,40]. It was reported that the aggregate size distribution of the filler network is stable during deformation, while an agglomerate breakdown occurs leading to the stress softening of the compound. It is known that the degree of branching and complexity of the space filling three-dimensional aggregate structure increases with higher surface area of the silica filler [8]. Consequently, the agglomerates become larger and more complex due to the entanglement of the highly branched aggregates, but at the same time, these structures are more fragile and prone to breakdown during strain as found in our study (Fig. 8a). The TEM analysis in Fig. 6 shows only a slight change in dispersion of the hydrophilic silica with higher specific surface area and therefore it can be assumed that agglomerates still exist in the compound contributing to energy loss and permanent set. Interestingly, the permanent set is almost independent of the surface treatment indicating a more important role of the agglomeration than filler-polymer interactions for irreversible structural changes. The structure modified AE R 8200 reveals the highest dispersion and forms probably aggregates and agglomerates of low complexity and small size leading to improved mechanical stability during deformation of the silicone compound (Fig. 8b). As also shown in literature, the hydrophobic surface treated by HMDS is beneficial for a uniform dispersion of silica fillers in compounds [41]. The consequence of high dispersion into small and stable agglomerates AE R 8200 leads to the lowest energy loss and permanent set even at high loading ratio.

4. Conclusions

Correlations based on synthetic fumed silicas specific surface area, aggregate morphology, surface modifications, processing aid and loading level were highlighted and discussed for HCR using hardness and Mullins testing. All mentioned factors have direct impact on hardness, energy loss and permanent set. It is found that with stronger filler-polymer interactions of hydrophilic silica without processing aid at high loading levels, the energy loss is significantly increased. The energy loss is lowered by either adding a processing aid or by hydrophobization of

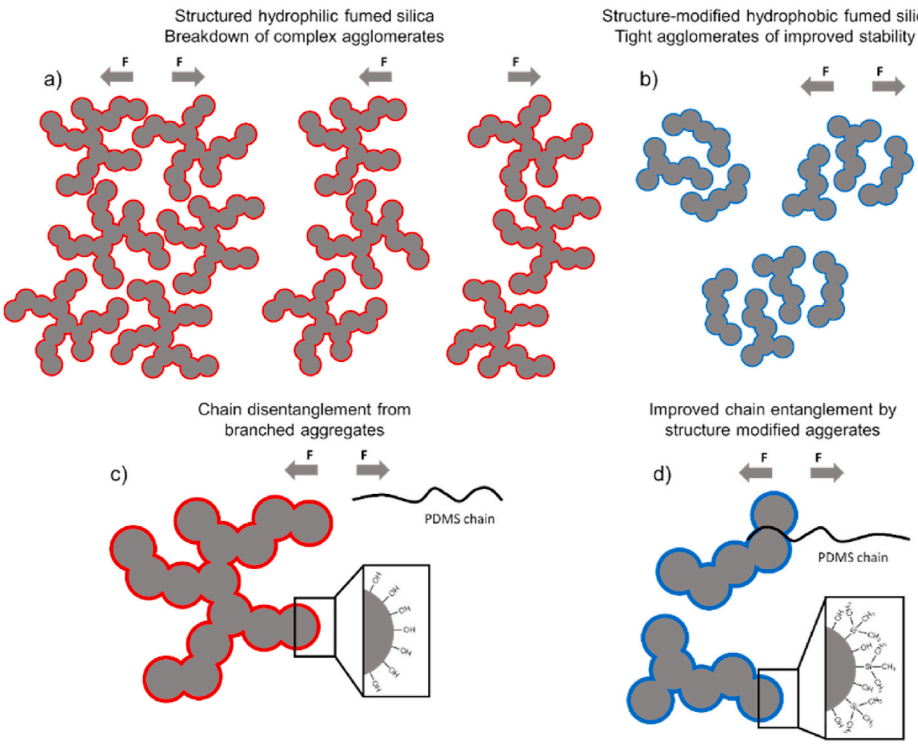

Fig. 8. Schematic illustration of the role of aggregate and agglomerate morphology as well as surface chemistry on stress softening for a,c) structured hydrophilic and b,d) structure modified hydrophobic fumed silica. The high branching of the structured hydrophilic aggregates leads to large agglomerates that are prone to breakdown during deformation a), while the small aggregates of the structure modified silica pack tightly in more mechanically stable agglomerates reducing the permanent set b). Additionally, as illustrated in c) and d) ruptures in filler-polymer interactions occur during deformation. For the structure modified hydrophobic filler chain, disentanglement is significantly reduced due to a lowered aggregate morphology.

the surface reducing the filler-polymer interactions and the corresponding ruptures during initial cyclic loading. Interestingly, the permanent set as a measure for structural breakage is almost independent of the surface modification of the filler indicating an important role of the aggregate and agglomerate morphology. Structured silica forms branched aggregates that assemble into complex agglomerates. During initial deformation of the silicone compound, the fragile agglomerates breakdown into smaller entities resulting in irreversible permanent set. To overcome these crucial disruptions and to minimize the permanent set, while ensuring good reinforcement, low structured and hydrophobic AEROSIL® R 8200 was applied. Former studies reported that this filler grade shows reduced chain adsorption at the silica surface and a lower chain entanglement at the decreased particle morphology, what is also related to an improved dispersion state as proven by our TEM analysis [42]. Furthermore, the low aggregate morphology of AEROSIL® R 8200 prevents the agglomerate breakage in contrast to the structured silica. These observations confirm that the combination of the hydrophobic surface treatment and structure modification of the silica diminishes structural ruptures and Mullins stress softening in filled elastomer composites. These guidelines for a rational design of filler particles is a general strategy for the improvement of the fatigue resistance of reinforced elastomer composites.

Author statement

Vincent Allen: Writing – original draft, Visualization, Data curation, Investigation, Methodology, Formal analysis. Lunhan Chena: Investigation, Methodology, Writing – review & editing. Milena Englert: Investigation, Methodology, Data curation, Writing – review & editing. Aziz Moussaoui: Project administration, Writing – review & editing. Wojciech Pisula: Conceptualization, Supervision, Visualization, Writing – review & editing.

Declaration of competing interest

The authors declare that they have no known competing financial interests or personal relationships that could have appeared to influence the work reported in this paper.

Acknowledgements

The authors would like to thank Dr. Victor Lifton and Frank Minister for their helpful discussions and valuable comments on the manuscript.

Appendix A. Supplementary data

Supplementary data to this article can be found online at https://doi.org/10.1016/j.compscitech.2021.108955.

References

[1] K. Brüning, In-situ Structure Characterization of Elastomers during Deformation and Fracture, Springer International Publishing, Berlin, 2014.
[2] C.M. Murphy, C.E. Saunders, D.C. Smith, Thermal and oxidation stability of polymethylphenylsiloxanes, Ind. Eng. Chem. 42 (1950) 2462–2468.
[3] D. Sharma A, Handbook of Analytical Inorganic Chemistry, first ed., International Scientific Publishing Academy, New Delhi, 2005.
[4] H.-D. Luginsland, J. Fröhlich, A. Wehmeier, Influence of different silanes on the reinforcement of silica-filled rubber compounds, Rubber Chem. Technol. 75 (2002) 563–579.
[5] A.M. Stricher, R.G. Rinaldi, C. Barres, F. Ganachaud, L. Chazeau, How I met your elastomers: from network topology to mechanical behaviours of conventional silicone materials, RSC Adv. 5 (2015) 53713–53725.
[6] L. Meunier, G. Chagnon, D. Favier, L. Orgéas, P. Vacher, Mechanical experimental characterisation and numerical modelling of an unfilled silicone rubber, Polym. Test. 27 (2008) 765–777.
[7] N. Hewitt, Compounding Precipitated Silica in Elastomers, William Andrew Publishing, 2007.
[8] A. Mulderig, G. Beaucage, K. Vogtt, H. Jiang, V. Kuppa, Quantification of branching in fumed silica, J. Aerosol Sci. 109 (2017) 28–37.
[9] H.K. Kammler, G. Beaucage, R. Mueller, S.E. Pratsinis, Structure of flame-made silica nanoparticles by ultra-small-angle X-ray scattering, Langmuir 20 (2004) 1915–1921.
[10] S. Wolff, J.-B. Donnet, Characterization of fillers in vulcanizates according to the einstein-guth-gold equation, Rubber Chem. Technol. 63 (1990) 32–45.
[11] P. Mazurek, S. Vudayagiri, A.L. Skov, How to tailor flexible silicone elastomers with mechanical integrity: a tutorial review, Chem. Soc. Rev. 48 (2019) 1448–1464.
[12] D.J. Kohls, G. Beaucage, Rational design of reinforced rubber, Curr. Opin. Solid State Mater. Sci. 6 (2002) 183–194.

[13] J. Fröhlich, W. Niedermeier, H.-D. Luginsland, The effect of filler-filler and filler-elastomer interaction on rubber reinforcement, Composites Part A Appl. Sci. Manuf. 36 (2005) 449–460.
[14] G. Heinrich, M. Klüppel, T.A. Vilgis, Reinforcement of elastomers, Curr. Opin. Solid State Mater. Sci. 6 (2002) 195–203.
[15] C.G. Robertson, M. Rackaitis, Further consideration of viscoelastic two glass transition behavior of nanoparticle-filled polymers, Macromolecules 44 (5) (2011) 1177–1181.
[16] A. Nakatani, W. Chen, R. Schmidt, G. Gordon, C. Han, Chain dimensions in polysilicate-filled poly (dimethyl siloxane), Polymer 42 (2001) 3713–3722.
[17] L.M. Guo, Y.A. Lv, Z.F. Deng, Y. Wang, Effect of strain rate on tension response of filled silicone rubber, Appl. Mech. Mater. 863 (2017) 112–116.
[18] J. Royo, Fatigue testing of rubber materials and articles, Polym. Test. 11 (1992) 325–344.
[19] J.L. Leblanc, Rubber-filler interactions and rheological properties in filled compounds, Prog. Polym. Sci. 27 (2002) 627–687.
[20] A.R. Payne, The dynamic properties of carbon black-loaded natural rubber vulcanizates. Part I, J. Appl. Polym. Sci. 6 (1962) 57–63.
[21] L. Mullins, Softening of rubber by deformation, Rubber Chem. Technol. 42 (1969) 339–362.
[22] J. Diani, B. Fayolle, P. Gilormini, A review on the Mullins effect, Eur. Polym. J. 45 (2009) 601–612.
[23] F. Clément, L. Bokobza, L. Monnerie, On the Mullins effect in silica filled polydimethylsiloxane networks, Rubber Chem. Technol. 74 (2001) 846–870.
[24] D.E. Hanson, M. Hawley, R. Houlton, K. Chitanvis, P. Rae, E.B. Orler, D. A. Wrobleski, Stress softening experiments in silica-filled polydimethylsiloxane provide insight into a mechanism for the Mullins effect, Polymer 46 (2005) 10989–10995.
[25] G. Machado, G. Chagnon, D. Favier, Induced anisotropy by the Mullins effect in filled silicone rubber, Mech. Mater. 50 (2012) 70–80.
[26] J.M. Clough, C. Creton, S.L. Craig, R.P. Sijbesma, Covalent bond scission in the Mullins effect of a filled elastomer: real-time visualization with mechanoluminescence, Adv. Funct. Mater. 26 (2016) 9063–9074.
[27] S. Krpovic, K. Dam-Johansen, A.L. Skov, Importance of Mullins effect in commercial silicone elastomer formulations for soft robotics, J. Appl. Polym. Sci. (2020), e50380.
[28] Z. Liao, M. Hossain, X. Yao, R. Navaratne, G. Chagnon, A comprehensive thermo-viscoelastic experimental investigation of Ecoflex polymer, Polym. Test. 86 (2020) 106478.
[29] D. Liu, L. Song, H. Song, J. Chen, Q. Tian, L. Chen, L. Sun, A. Lu, C. Huang, G. Sun, Correlation between mechanical properties and microscopic structures of an optimized silica fraction in silicone rubber, Compos. Sci. Technol. 165 (2018) 373–379.
[30] M. Tsige, T. Soddemann, S.B. Rempe, G.S. Grest, J.D. Kress, M.O. Robbins, S. W. Sides, M.J. Stevens, E. Webb III, Interactions and structure of poly (dimethylsiloxane) at silicon dioxide surfaces: electronic structure and molecular dynamics studies, J. Chem. Phys. 118 (2003) 5132–5142.
[31] M.I. Aranguren, E. Mora, C.W. Macosko, Compounding fumed silicas into polydimethylsiloxane: bound rubber and final aggregate size, J. Colloid Interface Sci. 195 (1997) 329–337.
[32] B.B. Boonstra, H. Cochrane, E.M. Dannenberg, Reinforcement of silicone rubber by particulate silica, Rubber Chem. Technol. 48 (1975) 558.
[33] Y. Yue, H. Zhang, Z. Zhang, Y. Chen, Polymer–filler interaction of fumed silica filled polydimethylsiloxane investigated by bound rubber, Compos. Sci. Technol. 86 (2013) 1–8.
[34] Y. Yue, H. Zhang, Z. Zhang, Y. Chen, Tensile properties of fumed silica filled polydimethylsiloxane networks, Composites Part A 54 (2013) 20–27.
[35] A. Camenzind, T. Schweizer, M. Sztucki, S.E. Pratsinis, Structure & strength of silica-PDMS nanocomposites, Polymer 51 (2010) 1796–1804.
[36] D. Mariot, A.-S. Caro-Bretelle, P. Ienny, F. Ganachau, Influence of the grafting topology of hydrophobic silica surfaces on the mechanical properties of silicone high consistency rubbers, Polym. Int. 64 (2015) 1128–1134.
[37] G. Kraus, C.W. Childers, K.W. Rollmann, Stress softening in carbon black-reinforced vulcanizates. Strain rate and temperature effects, J. Appl. Polym. Sci. 10 (1966) 229–244.
[38] M. Klüppel, J. Schramm, A generalized tube model of rubber elasticity and stress softening of filler reinforced elastomer systems, Macromol. Theory Simul. 9 (2000) 742–754.
[39] Y. Shui, L. Huang, C. Wei, J. Chen, L. Song, G. Sun, A. Lu, D. Liu, Intrinsic properties of the matrix and interface of filler reinforced silicone rubber: an in situ Rheo-SANS and constitutive model study, Compos. Commun. 23 (2021) 100547.
[40] M. Staropoli, D. Gerstner, M. Sztucki, G. Vehres, B. Duez, S. Westermann, D. Lenoble, W. Pyckhout-Hintzen, Hierarchical scattering function for silica-filled rubbers under deformation: effect of the initial cluster distribution, Macromolecules 52 (2019) 9735–9745.
[41] Q. Tian, C. Zhang, Y. Tang, Y. Liu, L. Niu, T. Ding, X. Li, Z. Zhang, Preparation of hexamethyl disilazane-surface functionalized nano-silica by controlling surface chemistry and its “agglomeration-collapse” behavior in solution polymerized styrene butadiene rubber/butadiene rubber composites, Compos. Sci. Technol. 201 (2021) 108482.
[42] T. Hanemann, D.V. Szabó, Polymer-Nanoparticle composites: from synthesis to modern applications, Materials 3 (2010) 3468–3517.